LUNAR TOPOGRAPHY AND THE LIMB COMPRESSION SOURCE REGIONS*†

L. J. SRNKA
Lunar Science Institute, Houston, Tex., U.S.A.
D. R. CRISWELL
Lunar Science Institute, Houston, Tex., U.S.A.
and
W. R. WOLLENHAUPT
NASA-Johnson Space Center, Houston, Tex., U.S.A.

Abstract. Data from the Apollo 15, 16, and 17 laser altimeters has been used to study slopes, elevations and roughness in the identifiable regions on the Moon which sporadically produce plasma compressions and magnetic field enhancements in the solar wind/lunar void boundary, when those regions are at a flow limb. It is found that occurrence rates for such 'limb compressions' derived from Explorer 35 satellite measurements are significantly correlated with peak, average and rms slopes in the source regions, whereas rates derived from Apollo 15 and 16 subsatellite data are not correlated with topography. This suggests that two or more mechanisms operate in the source regions to produce limb compressions. Together with the known correlation between limb compressions and local surface remanent magnetic fields, the results indicate that lunar magnetization is not strongly related to surface features.

1. Introduction

A number of identifiable areas on the lunar surface are sources of plasma compressions and magnetic field enhancements in the solar wind/lunar void boundary region when the area in question is positioned at the flow limb (Mihalov *et al.*, 1971; Sonett and Mihalov, 1972). These solar wind disturbances have been detected from 0.3 to 4.7 R_M (lunar radii) downstream from the limb by the Explorer 35 lunar orbiting spacecraft (Ness *et al.*, 1968; Taylor *et al.*, 1968; Siscoe *et al.*, 1969; Colburn *et al.*, 1971; Sonett and Mihalov, 1972), and at 100 km ($\sim 0.06\ R_M$) above the lunar surface by the Apollo 15 and 16 subsatellites (Sharp *et al.*, 1973; Russell *et al.*, 1973a, b, 1974; Russell and Lichtenstein, 1975). These disturbances are alternately referred to as penumbral increases (Ness *et al.*, 1968), external maxima (Colburn *et al.*, 1971), limb shocks (Criswell, 1973a, b), and limb compressions (Russell and Lichtenstein, 1975). The nomenclature 'limb compression' seems to be the most appropriate, and is adopted in this study.

Although limb compressions were a relatively minor feature in the early Explorer 35 observations of the solar wind/Moon interaction, their detection has prompted

* Paper presented at the Conference on 'Interactions of the Interplanetary Plasma with the Modern and Ancient Moon', sponsored by the Lunar Science Institute, Houston, Texas and held at the Lake Geneva Campus of George Williams College, Wisconsin, between September 30 and October 4, 1974.

† Lunar Science Institute Contribution, No. 212. The Lunar Science Institute is operated by the Universities Space Research Association under Contract No. NSR 09-051-001 with the National Aeronautics and Space Administration.

The Moon **14** (1975) 59–69.

considerable research on a range of lunar problems. See the recent work by Schubert and Lichtenstein (1974) for a review. The key issue in this subject remains the physical nature of the mechanism(s) which operate(s) in the source regions at or near the lunar surface to disturb the surrounding plasma and produce limb compressions in the streaming solar wind. There are a number of candidate mechanisms, including deflection by remanent magnetic fields (Barnes *et al.*, 1971) or the lunar atmosphere (Siscoe and Mukherjee, 1972; Wallis, 1974), local plasma heating by energetic photoelectrons (Criswell, 1973a, b), thermoviscous effects in an MHD boundary layer (Perez-de-Tejada, 1973), particle-kinetic effects (Whang, 1968; Ness *et al.*, 1968), and deflection by magnetic fields induced in the Moon by an electromagnetic interaction with the solar wind (Hollweg, 1968, 1970; Schwartz *et al.*, 1969). Some of these candidates are no longer contenders, and the remanent magnetic fields model is gaining favor (Russell and Lichtenstein, 1975). If it is shown that limb compressions are entirely due to solar wind interaction with local remanent magnetic fields, then the source region maps produced by Sonett and Mihalov (1972) and Russell and Lichtenstein (1975) essentially depict the intensity of lunar surface magnetization. However, the issue is not yet settled.

We present here an analysis of some relationships between lunar topography, based on Apollo laser altimetry, and the limb compression occurrence rates in the source regions. Some topographic control of occurrence rate is found. The implications of the correlation results for possible source mechanisms is discussed.

2. Laser Altimetry and Topography

A pulsed laser altimeter was used on the Apollo 15, 16, and 17 missions to measure the altitude of the CSM above the lunar surface (Kaula *et al.*, 1972, 1973, 1974; Roberson and Kaula, 1972; Wollenhaupt and Sjogren, 1972; Wollenhaupt *et al.*, 1973). A total of 4973 data points were obtained. The absolute uncertainty in the radial position of the instrument from the center of mass of the Moon is about 400 m, due primarily to uncertainties in the gravity field model (Kaula *et al.*, 1974). However, the data is more

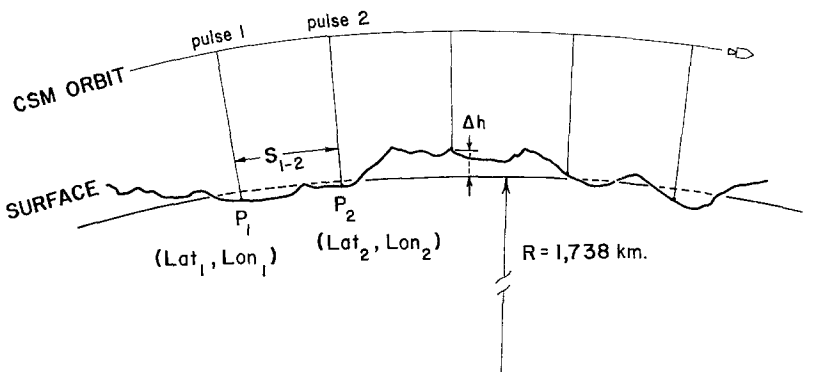

Fig. 1. Model geometry for calculating slopes and relief height from laser altimetry.

consistent internally, with ~ 10 m uncertainty in the relative radial positions of successive points along the same track. The sampling interval along the tracks was 30–43 km, and the laser spot size on the surface is estimated to be 30 m (Sjogren and Wollenhaupt, 1973).

The laser data used here consist of the measured deviations in surface elevation from a 1738 km sphere about the lunar center-of-mass, corrected for the CSM orbit and gimbal angles. The data was sorted into $15° \times 15°$ selenographic bins, from 30°N to 30°S and extending around the equator. The following parameters were calculated from the data points in each bin: maximum slope (absolute value), average sunrise-facing slope, average sunset-facing slope, root-mean-square (rms) slope, and average relief height above the mean Moon. The maximum relief height, minimum relief height, and relief height of the maximum slope were also recorded.

Figure 1 shows the model geometry used in the calculations. The separation S_{1-2} between laser points p_1 and p_2 which have selenographic coordinates $(\mathrm{LAT}_1, \mathrm{LON}_1)$ and $(\mathrm{LAT}_2, \mathrm{LON}_2)$ and elevation residuals Δh_1 and Δh_2 ,respectively, is roughly given by

$$S_{1-2} = \sin^{-1}\left[\frac{\sin\left(\frac{90 - \mathrm{LAT}_1}{180/\pi}\right)\sin\left(\frac{\mathrm{LON}_2 - \mathrm{LON}_1}{180/\pi}\right)}{\sin(A)}\right] R_{1-2}\,(\mathrm{km}),$$

where

$$A \equiv \tan^{-1}\left[\frac{\mathrm{cotan}\left(\frac{\mathrm{LON}_2 - \mathrm{LON}_1}{360/\pi}\right)\cos\left(\frac{\mathrm{LAT}_2 - \mathrm{LAT}_1}{360/\pi}\right)}{\cos\left(\frac{180 - (\mathrm{LAT}_1 + \mathrm{LAT}_2)}{360/\pi}\right)}\right] +$$

$$+ \tan^{-1}\left[\frac{\mathrm{cotan}\left(\frac{\mathrm{LON}_2 - \mathrm{LON}_1}{360/\pi}\right)\sin\left(\frac{\mathrm{LAT}_2 - \mathrm{LAT}_1}{360/\pi}\right)}{\sin\left(\frac{180 - (\mathrm{LAT}_1 + \mathrm{LAT}_2)}{360/\pi}\right)}\right],$$

and

$$R_{1-2} \equiv \frac{(\Delta h_1 + \Delta h_2)}{2} + 1738.$$

The slope SL_{1-2} between p_1 and p_2 is then given by

$$SL_{1-2} = \tan^{-1}\left(\frac{\Delta h_2 - \Delta h_1}{S_{1-2}}\right)\frac{180}{\pi} \quad (\text{degrees}).$$

Average slopes and elevations, standard deviations from the averages, and rms values are calculated using all points in a given bin, in the usual way.

Figure 2 shows the laser altimeter coverage. The analysis and results presented here are restricted to the 62 lunar bins which contain 14 or more data points each. The bin size was chosen to be compatible with the limb compression source region

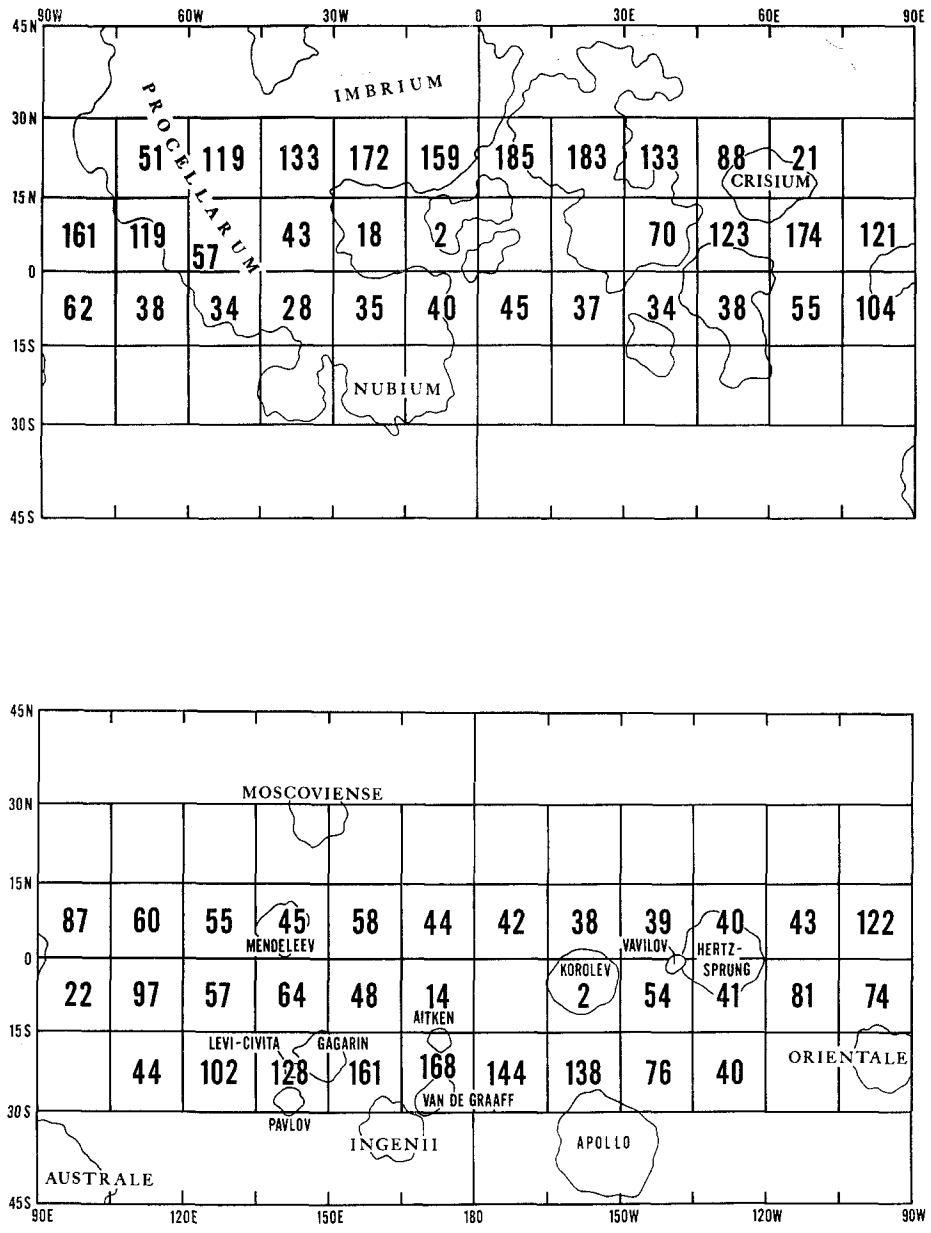

Fig. 2. Laser altimeter coverage of the lunar surface from Apollo 15, 16, and 17, quantized in 15° × × 15° bins. Large numerals indicate number of points in each bin.

maps (Sonett and Mihalov, 1972; Russell and Lichtenstein, 1975), so that the limb compression occurrence rates could be directly compared with topographic parameters.

3. Limb Compression Occurrence Rates

The occurrence rate r_s assigned to a given surface region is simply defined as the number of events attributed to that region, divided by the total number of observations for that region (i.e., $0 \lesssim r_s \lesssim 1$). Both the Explorer 35 and subsatellite data sets contain r_s values derived from measurements taken when the Moon was in the solar wind. However, the definition of a limb compression is slightly different in the two analyses.

Mihalov *et al.* (1971) and Sonett and Mihalov (1972) define a limb compression using the Ames magnetometer on Explorer 35 as an increase of at least 0.7γ above the average solar wind field. The increase is also required to be clean and free of obvious secondary perturbations. This value represents a minimum increase of only 10–20% above the background field, but since observations are made from as far as 4.7 R_M downstream, and since the amplitude of the perturbation is known to decrease with increasing downstream distance (Whang and Ness, 1972), the selection of such small perturbations is probably justified. Russell and Lichtenstein (1975) are more conservative in their definition, requiring that the subsatellites sense an increase of at least 50% over the upstream field, and that the upstream field exceeds 4γ and is reasonably steady. At least part of this conservatism is due to the observation of lunar remanent fields in excess of 1γ at the subsatellite altitudes (Russell *et al.*, 1973a, b), when the Moon is in the geomagnetic tail.

A second difficulty arises in the difference in selenographic resolution of the two data sets. Because of the higher Explorer 35 altitude, and the absence of plasma data for some magnetic field enhancements, r_s values can be assigned to bins no smaller than $15° \times 15°$ in this case. The lower subsatellite altitudes provide much better resolution, and so $5° \times 5°$ bins are used for mapping r_s values from the subsatellite measurements. In order to compare the two data sets, the subsatellite r_s values were combined, on a per unit area basis, to give equivalent values for $15° \times 15°$ bins. That is, the occurrence rate $(r_s)_A$ averaged from n smaller bins is

$$(r_s)_A \equiv \frac{\sum_{i=1}^{n} A_i (r_s)_i}{\sum_{i=1}^{n} A_i},$$

where A_i are the respective areas of the smaller bins. Since each r_s value is in fact mapped as a range in r_s (e.g. $0.20 \leqslant r_s \leqslant 0.49$ for subsatellite data), the mean value of r_s in that range is used in each case. The uncertainty in r_s is then one-half of that range, and this uncertainty is carried through the above calculation to give estimates of the uncertainty in the smoothed $(r_s)_A$ value. In this way 29 of the 62 bins containing

topographic parameters from the laser altimetry were assigned r_s values from the subsatellite data. All 62 bins have an associated r_s value from the Explorer 35 measurements.

4. Correlations

The mean r_s value for each bin was plotted as a function of six topographic parameters, for both subsatellite and Explorer 35 values of r_s. A best-fit linear regression analysis (method of least squares) was performed for each of the twelve plots. The significance of the correlation coefficient ϱ for each regression was examined with a two-tailed Student's t test. The hypothesis $\varrho=0$ was tested using the 5% level of significance, for df (degree of freedom)$=N-2=60$ for the Explorer data and df$=27$ for the subsatellite data. That is, at the calculated value of ϱ for a given plot, the probability that the correlation is random is less than 1 in 20 if $t>t_{0.05}$. The results are shown in Table I.

No correlation was found between the subsatellite r_s values and any topographic parameter in the bins. The same is true of Explorer 35 r_s values vs. relief heights. How-

TABLE I

Correlation statistics for limb compression occurrences vs six lunar topographic parameters derived from Apollo laser altimetry

	TOPOGRAPHIC PARAMETER	CORRELATION COEFFICIENT	VARIANCE PERCENTAGE	$t_{.05}$	STUDENTS t	SIGNIFICANT
EXPLORER 35 r_s vs	MAXIMUM SLOPE	0.601	36.14	2.000	5.827	YES
	AVE. SUNRISE SLOPE	0.611	37.33	2.000	5.979	YES
	AVE. SUNSET SLOPE	0.656	43.01	2.000	6.730	YES
	RMS SLOPE	0.639	40.91	2.000	6.445	YES
	MAX. RELIEF HEIGHT	0.074	0.55	2.000	0.575	NO
	AVE. RELIEF HEIGHT	0.166	2.77	2.000	1.309	NO
SUBSATELLITES r_s vs	MAXIMUM SLOPE	0.221	4.89	2.052	1.178	NO
	AVE. SUNRISE SLOPE	0.227	5.19	2.052	1.216	NO
	AVE. SUNSET SLOPE	0.266	7.10	2.052	1.437	NO
	RMS SLOPE	0.263	6.93	2.052	1.418	NO
	MAX. RELIEF HEIGHT	0.232	5.39	2.052	1.241	NO
	AVE. RELIEF HEIGHT	0.100	1.01	2.052	0.524	NO

ever, significant correlations exist between the average limb compression occurrence rates deduced from Explorer 35 data and the maximum, ave. sunrise, ave. sunset, and rms slopes in the bin which contains the source region. The best correlation of these is r_s vs average sunset-facing slope, where more than 43% of the variation in r_s values is directly due to a linear dependence on slope (i.e. the variance percentage).

The difference between the Explorer 35 and subsatellite correlation results is puzzling. Typical examples of the above plots are shown in Figures 3a (Explorer 35) and 3b (subsatellite). Notable topographic features are indicated on each figure, and the regression line is shown for the Explorer 35 data. Note the disagreement in average r_s values for the same bin (i.e. feature) in the two figures. Some of this discrepancy may be due to different definitions of 'limb compression' between experimenters, as mentioned earlier. But for the Levi-Civita, Gagarin, and Apollo crater regions the disagreement is more than a factor of 3, which seems too large to account for in this way. Rather we suggest here that the correlation differences are the result of the difference in orbital altitudes between the subsatellites and Explorer 35 at which the limb compressions were detected. For example, part of the lack of correlation with the

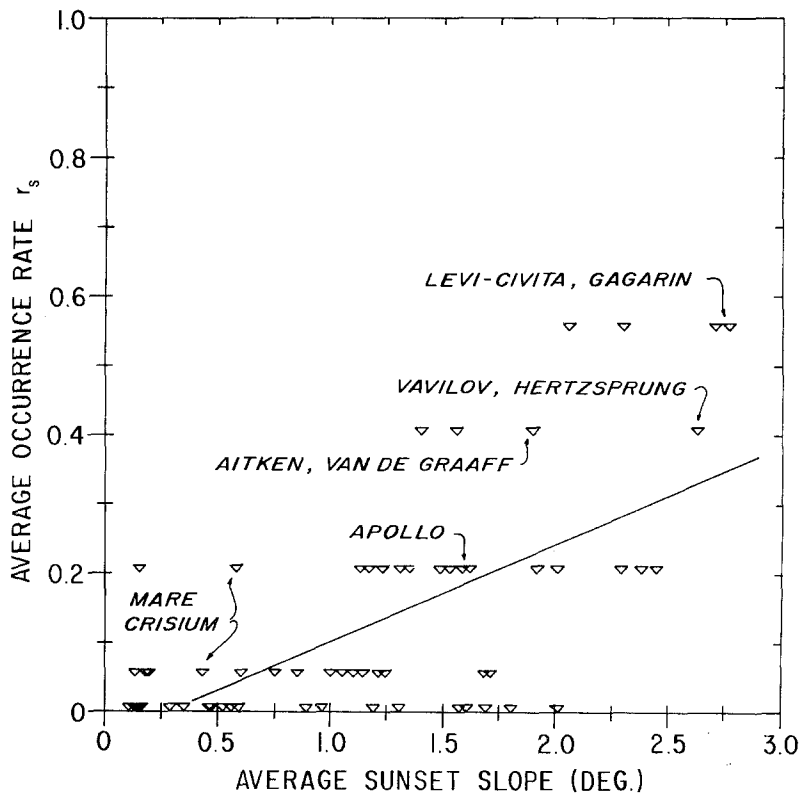

Fig. 3a. Correlation of limb compressions detected by Explorer 35 with slope in the source region. The data for r_s vs max. slope, ave. sunrise slope, and rms slope are similar. Typical uncertainty in r_s is $\pm 25\%$.

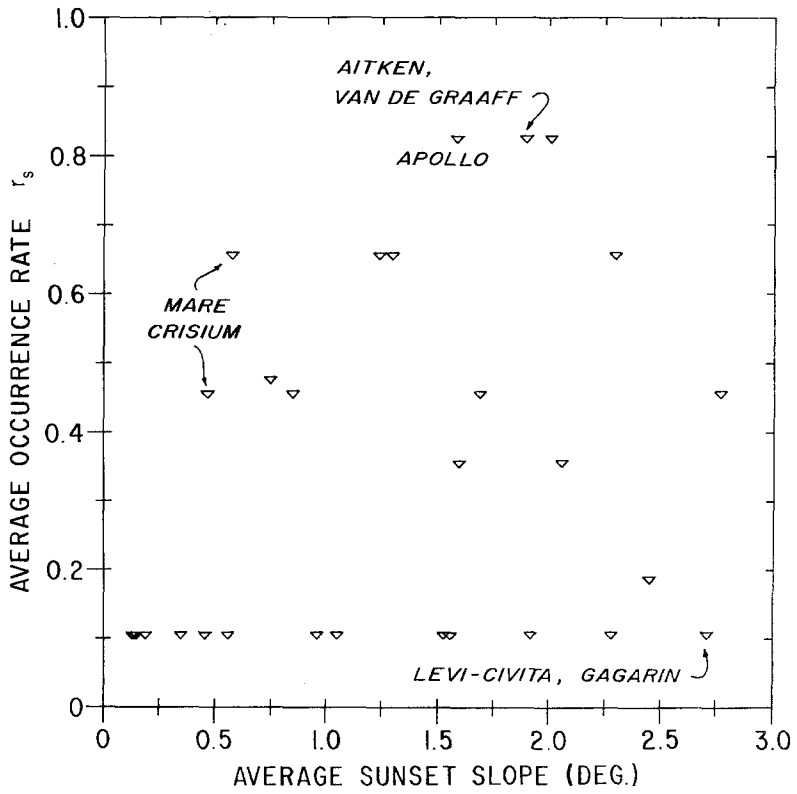

Fig. 3b. Apollo 15 and 16 subsatellite occurrence rate data. The large scatter appears in all six attempts to correlate r_s with topography.

subsatellite data may be due to the maximization of strong limb compressions ($\approx 20\gamma$) at least 10° upstream of the limb (Russell and Lichtenstein, 1975).

If some fraction of the events detected by Explorer 35 do not fully develop until the flow is 0.1–0.2 R_M downstream from the limb, these occurrences would not be seen by the subsatellites. Conversely, if some limb compressions rapidly dissipate in the solar wind, the 0.7γ criterion may not be met downstream at the Explorer 35 distance and no occurrence would be registered there. The plasma physics of such processes is complex, and much additional work is needed before definitive replies can be given to these speculations. But it is instructive to consider how variations in possible source mechanisms among lunar regions could influence the limb compression occurrence rate.

5. Source Mechanisms

The correlation results in Table I show that in a given selenographic region the maximum slope, average slope, and rms slope (or degree of 'roughness') have considerable control of Explorer 35 r_s values. Two possible conclusions can be drawn.

If all limb compressions are due to the deflection of solar wind plasma by surface remanent magnetic fields, the magnetization must be correlated with topographic slopes and/or roughness. Alternatively, if only some of the occurrences are associated with remanent fields, the remainder must have a source mechanism which is dependent on slopes.

Russell and Lichtenstein (1975) have compared subsatellite r_s values and remanent field strengths measured at 100 km altitude when the Moon is in the geomagnetic tail. It is found that occurrence rate and field strength are directly correlated, at least in the two selenographic areas where the data sets overlap. If this relationship holds for the remainder of the regions where fields have been detected (cf. Russell *et al.*, 1974) as is likely, then the results in Table I for the subsatellite case imply that lunar remanent magnetization is not correlated with any of the six topograpfic parameters considered. This is an important result, and will be treated more fully in a later paper.

It therefore seems likely that the second alternative above is correct: namely, that limb compressions are caused by solar wind/remanent surface field interactions *and* one or more source mechanisms which are dependent on the slopes found in lunar terrain. Photoelectron heating of the solar wind at steep slopes ($>5°$) near the flow limbs is one possibility (Criswell, 1973a, b). Plasma turbulence generated by electron gyroradius effects at rough terrain on the flow limb may also have a role, although this is more uncertain. If the MHD boundary layer model (Perez-de-Tejada, 1973) is sensitive to surface roughnesss, some thermoviscous effects could be important, although the mechanisms of the energy transfer and the transfer rate itself are in some doubt.

The photoelectron model may explain the slope-dependent r_s values. This model recognizes that although the net charge flux to a unit surface area on the Moon is zero in the steady state (i.e., the Moon is electrically insulating), the net energy flux with respect to the solar wind is non-zero. Indeed, only under very fortuitous circumstances will the energy flux of plasma ions and electrons exactly balance the photoelectron energy flux into the wind. Both the magnitude and sign of the energy flux are dependent on solar photon and plasma fluxes, the photoemissive properties of the surface, and slope in a nonlinear way. At steep slopes near the terminator the energy flux can be positive outwards, primarily due to photoemission produced by solar photons with energies above 80 eV (Criswell, 1973a). Slopes approaching 11° with heights exceeding 5 km were found in this study of the laser altimetry, which in terms of the photoelectron model are ideal sources for the energy fluxes necessary to produce limb compressions.

It is reasonable to assume that the energetic photoelectrons are initially confined to an interplanetary magnetic field flux tube which extends about two photoelectron gyroradii above the surface, say <20 km for 80 eV. Thus subsatellite magnetometer data taken at 100 km altitude over such a region of photoelectron/plasma heating would record no limb compression. Both the subsatellites and Explorer 35 should detect these disturbances downstream, but the occurrence rate may be higher at Explorer 35 distances due to merging of heated flow elements, each of which could

have a separate surface source. Note that limb compressions attributed to remanent magnetic fields observable at 100 km altitude should be detected by both the subsatellites and Explorer 35. The r_s values for the Aitken-Van de Graaff region which has an extensive remanent field are similar for the two data sets, confirming this view.

6. Conclusions

Comparison of Apollo laser altimetry with subsatellite and Explorer 35 magnetometer data gives new insight into two lunar problems: the photoelectron/plasma environment near the surface, and the nature of the Moon's magnetic field. Limb compressions are related to both of these. At least two mechanisms must act as sources for these events: interaction of the solar wind with remanent magnetic fields, and one or more mechanisms which depend on surface slope at the flow limb. Photoelectron heating of the plasma adjacent to high, steep features near the terminator is proposed as the most likely slope-dependent source mechanism.

The Valivov/Hertzsprung crater region on the lunar farside has a high occurrence rate ($r_s=0.4\pm0.1$) determined from Explorer 35 data, but the remanent magnetic field at 100 km over this area is very weak (Russell *et al.*, 1974). Laser altimetry shows the area to be rough, with numerous features exceeding 5° in slope and 3 km in relief. This region is a good candidate source for photoelectron-generated limb compressions. Levi-Civita may be another example. On the other hand, Mare Crisium is active in the subsatellite limb compression data ($0.45<r_s<0.65$), but much less so in the Explorer 35 data ($0.05<r_s<0.2$). This area is relatively smooth, with average slope $<1°$. Limb compressions originating near Mare Crisium are likely caused by solar wind interaction with small-scale remanent magnetic fields.

There is no evidence in the laser altimetry that lunar remanent fields are significantly correlated with topography, except for the well-known nearside vs farside asymmetry. This suggests that the fields have sources which lie at some depth beneath the lunar surface. Since the vertical gradient in the remanent fields is quite large, and since the scale sizes of the fields decreases in proportion to the altitude (Russell *et al.*, 1975), the source depth is probably less than 100 km.

Acknowledgment

The Lunar Science Institute is operated by the Universities Space Research Association under Contract No. NSR 09-051-001 with the National Aeronautics and Space Administration. This paper constitutes the Lunar Science Institute Contribution No. 212. The authors thank D. C. Kinsler for preparation of the figures.

References

Barnes, A. P., Cassen, S. D., Mihalov, J. D., and Eviator, A.: 1971, *Science* **712**, 716–718.
Colburn, D. S., Mihalov, J. D., and Sonett, C. P.: 1971, *J. Geophys. Res.* **76**, 2940–2957.
Criswell, D. R.: 1973a, *The Moon* **7**, 202–238.

Criswell, D. R.: 1973b, in R. J. L. Grard (ed.), *Photon and Particle Interactions with Surfaces in Space*, D. Reidel, Dordrecht, p. 443.
Hollweg, J. V.: 1968, *J. Geophys. Res.* **73**, 7269–7276.
Hollweg, J. V.: 1970, *J. Geophys. Res.* **75**, 1209–1216.
Kaula, W. M., Schubert, G., Lingenfelter, R. E., Sjogren, W. L., and Wollenhaupt, W. R.: 1972, *Proc. Third Lunar Sci. Conf., Geochim. Cosmochim. Acta., Suppl. 8*, **3**, 2189–2204, MIT Press.
Kaula, W. M., Schubert, G., Lingenfelter, R. E., Sjogren, W. L., and Wollenhaupt, W. R.: 1973, *Proc. Fourth Lunar Sci. Conf., Geochim. Cosmochim. Acta., Suppl. 4*, **3**, 2811–2819, Pergamon.
Kaula, W. M., Schubert, G., Lingenfelter, R. E., Sjogren, W. L., and Wollenhapt, W. R.: 1974, *Proc. Fifth Lunar Sci. Conf., Geochim. Cosmochim. Acta., Suppl. 5*, **3**, 3049–3058, Pergamon.
Mihalov, J. D., Sonett, C. P., Binsack, J. H., and Moutsoulas, M. D.: 1971, *Science* **171**, 892–895.
Ness, N. F., Behannon, K. W., Taylor, H. E., and Whang, Y. C.: 1968, *J. Geophys. Res.* **73**, 3421–3440.
Perez-de-Tejada, H.: 1973, *J. Geophys. Res.* **78**, 1711.
Roberson, F. I. and Kaula, W. M.: 1972, *Apollo 15 Prelim. Sci. Report*, NASA Publ. SP-289, 25: 48–50.
Russell, C. T. and Lichtenstein, B. R.: 1975, *J. Geophys. Res.* in press.
Russell, C. T., Coleman, P. J., Jr., Lichtenstein, B. R., Schubert, G., and Sharp, L. R.: 1973a, *Space Research XIII*, 951–960, Akademie-Verlag.
Russell, C. T., Coleman, P. J., Jr., Lichtenstein, B. R., Schubert, G., and Sharp, L. R.: 1973b, *Proc. Fourth Lunar Sci. Conf., Geochim. Cosmochim. Acta, Suppl. 4*, **3**, 2833, Pergamon.
Russell, C. T., Coleman, P. J., Jr., Lichtenstein, B. R., Schubert, G., and Sharp, L. R.: 1974, *Space Research XIV*, 629, Akademic-Verlag.
Russell, C. T., Coleman, P. J., Jr., Fleming, B. K., Hilburn, L., Lichtenstein, B. R., and Schubert, G.: 1975, *Lunar Science VI*, part 2, 695, NASA-JSC and The Lunar Science Institute.
Schubert, G. and Lichtenstein, B. R.: 1974, *Rev. Geophys. Space Phys.* **12**, 592–626.
Schwartz, K., Sonett, C. P., and Colburn, D. S.: 1969, *The Moon* **1**, 7–30.
Sharp, L. R., Coleman, P. J., Jr., Lichtenstein, B. R., Russell, C. T., and Schubert, G.: 1973, *The Moon* **7**, 322–341.
Siscoe, G. L. and Mukherjee, N. R.: 1972, *J. Geophys. Res.* **77**, 6042.
Siscoe, G. L., Lyon, E. F., Binsack, J. H., and Bridge, H. S.: 1969, *J. Geophys. Res.* **74**, 59.
Sjogren, W. L. and Wollenhaupt, W. R.: 1973, *Science* **179**, 275–278.
Sonett, C. P. and Mihalov, J. D.: 1972, *J. Geophys. Res.* **77**, 588–603.
Taylor, H. E., Behannon, K. W., and Ness, N. F.: 1968, *J. Geophys. Res.* **73**, 6723.
Wallis, M. K.: 1974, *J. Geophys. Res.* **79**, 275–279.
Whang, Y. C.: 1968, *Phys. Fluids* **11**, 969.
Whang, Y. C. and Ness, N. F.: 1972, *J. Geophys. Res.* **77**, 1109–1115.
Wollenhaupt, W. R. and Sjogren, W. L.: 1972, *The Moon* **4**, 337–347.
Wollenhaupt, W. R., Sjogren, W. L., Lingenfelter, R. E., Schubert, H., and Kaula, W. M.: 1973, *Apollo 17 Preliminary Science Report*, NASA Publ. SP-315, 30: 1–5.